doi:10.20944/preprints201809.0176.v1

Peer-reviewed version available at *Life* **2018**, *8*, 42; doi:10.3390/life8040042

Article

Formamide Adsorption at the Amorphous Silica Surface: a Combined Experimental and Computational Approach

Matteo Signorile [1], Clara Salvini [1], Lorenzo Zamirri [1], Francesca Bonino [1], Gianmario Martra [1], Mariona Sodupe [2], Piero Ugliengo [1]*

[1] Dipartimento di Chimica and NIS, Università di Torino, Via P. Giuria 7 – 10125 Torino and Via G. Quarello 15/A – 10135 Torino, Italy

[2] Departament de Química, Universitat Autònoma de Barcelona, 08193 Bellaterra, Spain

* Correspondence: piero.ugliengo@unito.it; Tel.: +39-011-670-4596

Abstract: Mineral surfaces have been demonstrated to play a central role in prebiotic reaction, which are supposed to be at the basis of the origin of life. Among the various molecules proposed as precursors for these reactions, one of the most interesting is formamide. Formamide has been shown to be a pluripotent molecule, generating a wide distribution of relevant pre-biotic products. In particular, the outcomes of its reactivity are strongly related to the presence of mineral phases, acting as catalysts toward specific reaction pathways. Even if the mineral-products relationship has been deeply studied for a large pool of materials, the fundamental description of the formamide reactivity over the mineral surface at a microscopic level is missing in the literature. In particular, a key step of formamide chemistry at surfaces is its adsorption on the available interaction sites. This report aims to investigate the adsorption of formamide over a well-defined amorphous silica, chosen as model mineral surface. An experimental IR investigation of formamide adsorption has been carried out and its outcomes have been interpreted on the basis of first principles simulation of the process adopting a realistic model of the amorphous silica.

Keywords: formamide; silica; IR-spectroscopy; DFT

---

1. Introduction

The understanding of the origin of life under a chemical perspective is an emerging multidisciplinary topic in the last years. Originally developing in the astro- and bio-chemistry communities, nowadays it is spreading across other branches such as organic, physical and computational chemistry [1]. Due to the complexity of the subject, a multifaceted approach is indeed unavoidable. Several scenarios have been hypothesized in the last decades to describe the process leading from the simplest chemical moieties to biologically relevant molecules (e.g. nucleic acids, proteins, etc), by passing through their key building blocks such as amino-acids, nucleobases, sugars, fat acids, etc. The formation of these latter species from the simplest molecules ubiquitously found in our universe is the step where a fundamental chemical approach can give its utmost contribution.

Among the various pathways proposed, an interesting option relies on the polyhydric chemistry of formamide: as reported in several research papers [2–12], formamide is able to originate many relevant prebiotic molecules (and particularly nucleobases) under mild thermal or photochemical reaction conditions. Furthermore, the selectivity toward specific products is strongly affected by the presence of mineral phases in the reaction environment: it is logical to expect that the surfaces of these minerals can drive the reaction steps leading from the bare formamide to the final products, eventually also catalyzing some of these processes. Surprisingly, such effect on selectivity is observed also for extremely simple, earth abundant minerals, e.g. carbonates, aluminates, silicates, etc [10]. In the latter category, also the bare silica has been shown to drive the reactivity of formamide toward specific products (mostly purine and cytosine), whereas it has been found to be inert toward many industrially exploited chemical processes (where it is effectively exploited as catalyst support).

Even if the reactivity of formamide at the silica surface has been demonstrated and documented [13], a physico-chemical description of the fundamental steps of this process is missing in the literature. Such lack is not limited to the only study of the reactivity, but includes the study of the bare formamide-SiO_2 interaction (i.e. adsorption) too. Even if it can be considered straightforward, the study of formamide adsorption on silica presents some criticism that have to be addressed in order to provide a rigorous and clean description of the process. First of all, silica is a rather general label which describes thousands of different polymorphs, both crystalline and amorphous. Then, depending on the "chemical history" of each sample, surface properties (exposed faces, density of terminal hydroxyl groups, etc) can deeply vary on formally identical materials. A further complication arises from formamide, which is known to favorably form dimers, thus increasing the variability on the species reaching the surface in a typical gas-phase adsorption experiment. The combination of all the previous variables can potentially lead to a significant heterogeneity in experimental results: a precise experimental design is thus required, in order to get proper insight on the formamide adsorption process at silica. By reducing the variability of the system under study, its theoretical modelling is facilitated too, since well-defined systems are obviously easier to simulate with fully representative models.

In this work, we adopted the well-known Aerosil OX 50 (A50) pyrolitic silica as model. Despite its amorphous structure, A50 possesses a significant surface area (50 m^2g^{-1}, according to the producer) compared to commercially available crystalline SiO_2, still owning a relatively low surface concentration of hydroxyl groups, i.e. silanols. Through *ad hoc* thermal treatments [14], the population of the latter can be finely tuned toward a large prevalence of isolated silanols, thus giving rise to a well-defined surface. Accounting for these peculiarities, A50 represents an optimal model of silica in the framework of a fundamental adsorption study. Nevertheless, the IR spectra of formamide adsorbed at A50 revealed a heterogeneous behavior: on the basis of the only experiment, it is however impossible to ascribe these small spectral differences to the adsorption of formamide at slightly different sites and/or to different ways of interaction of the molecule at the same place at the surface. In order to fully elucidate the adsorption mechanisms, a computational study has been performed, aiming to predict the interaction at different sites with various molecules-surface reciprocal orientations. Furthermore, the effect of formamide loading has been considered by simulating single and double adducts. IR spectra have been simulated for each structure within the harmonic approximation and combined through a Boltzmann's weighted average to give a reconstruction of the experimental one.

2. Materials and Methods

2.1 Experimental approach

Aerosil 50 (A50) has been chosen as model amorphous silica, since it is a well-known material whose physico-chemical properties and interaction with several biologically relevant molecules have been studied in depth [15–17]. The pristine A50 has been preliminary treated in order to obtain a controlled and homogenous surface silanols distribution. The method proposed by Rimola et al. has been applied [14], thus exposing A50 to a two steps thermal activation in a static furnace. During the first step, the bare silica (in self-supported pellet form) has been heated to 450 °C with a rate of ~10 °C min^{-1}, maintaining the temperature for 2.5 h. Such procedures yield a silica surface with a final silanol density of ~1.5 isolated OH per nm^2 and with a negligible amount of interacting OH group. The already pelletized sample has been directly used in the in situ IR study of formamide adsorption. We adopted a home-made quartz glass spectroscopy cell with minimal optical path and equipped with KBr windows. After 0.5 h of outgassing at RT, the sample was exposed for 1 h to the vapor pressure (~1.5 mbar) of formamide at the same temperature. After this loading stage, the desorption of formamide from the silica surface upon outgassing at RT was monitored. IR spectra have been collected with a resolution of 2 cm^{-1} on a Bruker Vertex 70 Fourier-transform spectrometer, equipped

Peer-reviewed version available at Life 2018, 8, 42; doi:10.3390/life8040042

with a cryogenic Mercury-Cadmium-Telluride (MCT) detector operated at liquid N_2 temperature (77 K).

2.2 Computational approach

In order to simulate the adsorption of formamide over A50, a periodic 2-dimensional slab silica surface model, with hydroxylation similar to the experimental one (~1.5 OH/nm^2) has been derived. With respect to models previously proposed [13, 18–23], a thinner one has been adopted in this work: in detail, the thickness of the model previously proposed by Ugliengo et al. [19], has been stepwise reduced down to a single monolayer of SiO_2. On the cut side, the surface has been terminated by silane groups, keeping the position of terminal H fixed at the original coordinates of the former O atoms. The procedure is schematically highlighted in Figure 1.

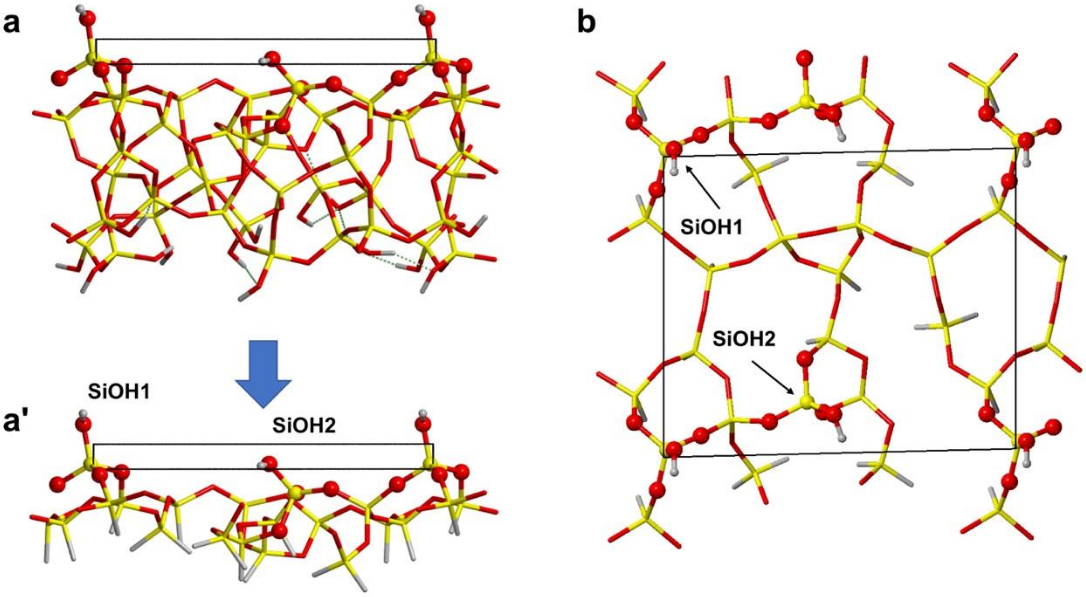

Figure 1. Side views of: a) reference SiO_2 model from Ref. [19]; and a') the derived thin SiO_2 model adopted in this work. b) top view of the thin SiO_2 model.

The resulting surface exhibits 58 atoms (including the 14 terminal H), with unit cell parameters a = 11.64 Å, b = 13.60 Å e γ = 88.65°, fixed at those optimized for the larger silica model, while the atomic coordinates of all atoms (but the terminal H atoms of the silane groups) were fully relaxed. The model sports two different isolated silanols, hereafter referred as SiOH1 and SiOH2 (see Figure 1). The main difference between these is represented by greater protrusion of SiOH1, whereas SiOH2 lays closer to the surface. We docked formamide to the silica surface in order to simulate the most relevant adsorption processes by maximizing H-bond interactions and fully optimized the coordinates of all atoms keeping the unit cell size fixed at that of the free silica slab (as well as the H atoms of the silane groups). Since these H-bond interactions usually fall in the energy range proper of physisorption, dispersive interactions compete in determining both the final structure and the extent of the interaction energy of each adduct and, ultimately, also the vibrational spectra [24]. Therefore, the final optimized structures result from a delicate balance between these two components of the interaction energy. Furthermore, since two different adsorption sites (i.e. silanols) are exposed in the unit cell, also coverage must be considered: for simplicity, we will refer to low coverage (LC) for a single formamide adsorbed on the surface and to high coverage (HC) when two molecules are adsorbed (i.e. formamide interacts with all silanols). Another relevant aspect, is that formamide dimerizes with high interaction energy [25, 26], thus the adsorption of dimeric species has also been considered. At our computational level (vide infra), the Gibbs free energy for the dimerization reaction in gas phase is -18 kJ mol^{-1}, testifying the prevalence of the dimeric over isolated formamide in gas-phase. Furthermore, at least two formamide molecules can adsorb

Peer-reviewed version available at Life 2018, 8, 42; doi:10.3390/life8040042

simultaneously at the surface, directly yielding a HC structure. Moreover, at HC condition the two formamide molecules can interact to each one with a silanol (in a "double-monomer" fashion) or they can give rise to adsorbed dimeric structures, with a strong molecule-molecule interaction, in the latter case. Figure 2 shows the general scheme accounting for all possible way in which formamide has been docked to the silica surface.

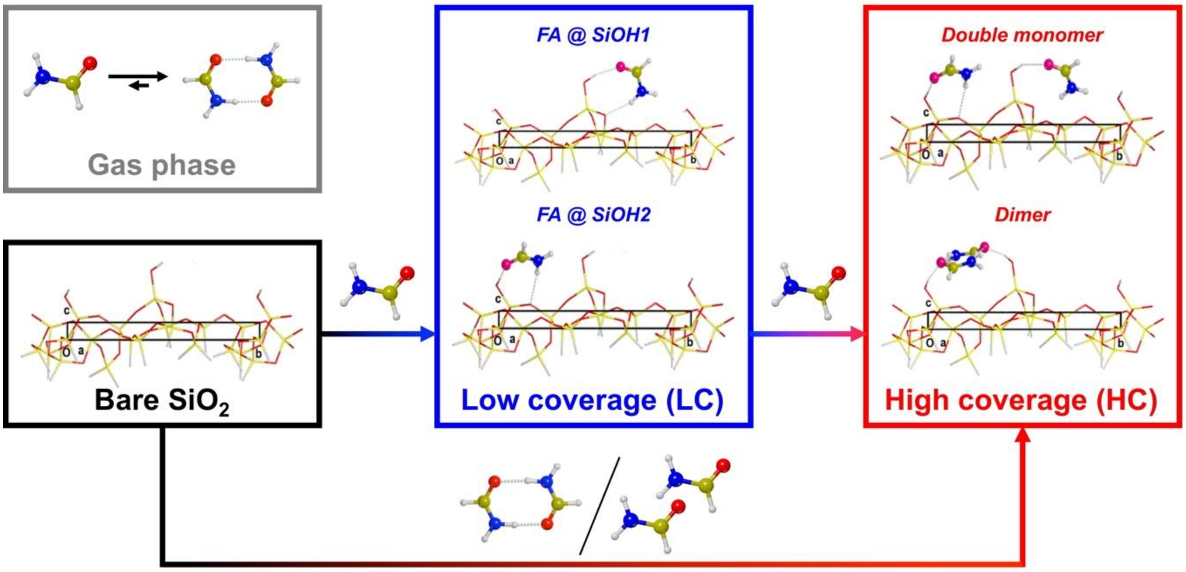

Figure 2. Scheme accounting for all cases considered of formamide adsorbed at the silica surface.

Since the complexity of the adsorption process, the study reported in this work has been limited to the simplest case of subsequent adsorption of single formamide molecules, according to the following processes (FA as formamide):

$$SiO_2 + FA \rightarrow SiO_2 \cdots FA \quad (1)$$

$$SiO_2 \cdots FA + FA \rightarrow SiO_2 \cdots 2(FA) \quad (2)$$

Interaction energies (ΔE), enthalpies (ΔH) and Gibbs (ΔG) free energies for all considered processes have been computed through the usual formula:

$$\Delta X = X_{products} - X_{reactants} \quad (3)$$

where $X = E$, H or G. Products refer to the right hand of equations 1) and 2) (adsorbed complexes), therefore the computed ΔX are all negative for bounded adducts at the silica surfaces.

According to this stepwise process, 12 adsorption processes were simulated, 5 LC and 7 HC (of which 4 dimeric and 3 double-monomeric structures). A detailed structural overview of all these models is given in the Supplementary Materials (Figures and Tables S1 to S12).

All the calculation presented in this work have been performed with the CRYSTAL17 code [27, 28], adopting the Perdew-Burke-Enzerhof (PBE) GGA functional for both correlation and exchange terms [29]. As basis set, Si and O atoms have been described through the polarized double-ζ quality basis set proposed by Nada et al. [30], whereas formamide (H, C, N, O) and terminal silane groups adopted the Ahlrichs VTZ (including polarization functions) basis set [31]. The electron density has been integrated over a pruned grid having 75 radial points and a maximum number of 974 angular (defined as XLGRID within the code). The truncation criteria for bi-electronic integrals, i.e. the TOLINTEG parameters, have been set to {7 7 7 7 16}, pursuing good accuracy. The diagonalization of the Hamiltonian matrix has been performed at Γ point only (SHRINK parameter set to {1 1}). The

Peer-reviewed version available at Life 2018, 8, 42; doi:10.3390/life8040042

Grimme D2 empirical scheme has been applied to take in account the effect of dispersive interactions [32]. As this term is simply added to the electronic energy, the purely dispersive contribution to the interaction energy ΔE (Eq. 3), was easily extracted. All the computational parameters not mentioned above have been left to the default values, according to the CRYSTAL17 manual [33]. Adsorption energies have been calculated after energy relaxation upon formamide adsorption and corrected for the basis set superposition error (BSSE) according to the counterpoise method [34]. Adsorption enthalpies, Gibbs free energies and vibrational frequencies for formamide (including IR intensities) have been estimated through a reduced Hessian approach, where the calculation has been limited to a fragment envisaging the adsorbed molecule(s) and the silanol groups (always all of them have been included in the fragment for which frequencies were computed, irrespective of their occupation by formamide). Vibrational frequencies for the C=O stretching and the NH$_2$ bending (as the main target of the experiments) have been scaled by two separate proportionality factors (0.9972 and 1.0102 respectively), derived from the ratio of experimental over calculated frequencies of the modes for the free formamide molecule [35]. This accounts for anharmonicity and facilitates a direct comparison with the experimental adsorption bands.

3. Results

3.1 FTIR of formamide adsorbed at A50

In Figure 3 the FTIR spectra of formamide adsorbed at the silica surface are reported in the most interesting spectral regions, i.e. where the carbonyl stretching and the X-H (X = C, N or O) stretching modes fall.

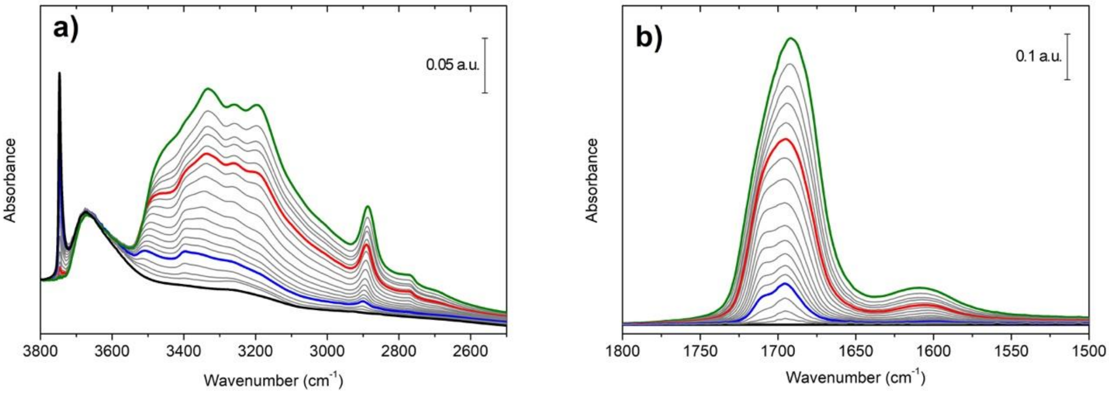

Figure 3. a) IR spectra of formamide adsorbed at the A50 surface in the X-H (X = C, N or O) stretching region; and b) baseline subtracted IR spectra of formamide adsorbed at the A50 surface in the carbonyl stretching region. The black curves refer to the bare silica outgassed 0.5 h at RT. The green curves refer to the maximum formamide coverage achieved after 1 h of exposure of silica to its vapor pressure (1.5 mbar) at RT. The red has been considered as HC reference spectrum. The blue curve has been selected as LC reference spectrum. The gray curves have been obtained during the outgassing of formamide at RT and their time evolution is from the green curves toward the black ones.

In the X-H (X = C, N or O) stretching modes region, looking at the spectrum before formamide contact (black curve of Figure 3a), the dominating feature is a sharp peak with maximum at 3748 cm^{-1}. This signal is straightforwardly ascribable to isolated silanols exposed at the silica surface. A second feature is represented by a broader band peaked at ~3675 cm^{-1}, testifying the presence of a fraction of silanols interacting through hydrogen bond. At maximum formamide dosage, the former signal is fully eroded, suggesting the molecule has a direct interaction with isolated silanols, as logically expected. Conversely, the latter band seems unperturbed upon adsorption, pointing out the related interacting silanols are not accessible by formamide: these are, most probably, intra-globular silanol nests, thus chains of hydrogen bonded silanols embedded in inaccessible internal cavities of the silica particles. Another relevant feature observed at full coverage is a complex overlap of signals in the

3000-3500 cm^{-1} range, due to the formamide vibrational modes, also establishing hydrogen bonds with the SiO_2 surface and/or other formamide molecules.

Due to the effect of the hydrogen bond, the X-H band is very broad and poorly informative of the specific interaction with formamide. Its broadness indicates, anyhow, that H-bond is occurring between formamide and silanol groups at the surface, as expected. Different spectral windows are, therefore, more effective in characterizing the interacting formamide. In this regard, the observation of the carbonyl stretching region is much more informative. This latter range at maximum coverage (red curve of Figure 3b) is characterized by the presence of a complex band centered at approximately 1690 cm^{-1}, most probably arising from the overlap of more than a single component as suggested by its broad, asymmetric shape. Looking at the outgassing sequence, two distinct components can be recognized: the most intense one blue shifts from 1690 cm^{-1} up to 1695 cm^{-1} while coverage is reduced, whereas the second component appears as a shoulder at 1710 cm^{-1}, becoming more defined at lower coverages and whose frequency remains constant at every coverage. Both these signals can be related to carbonyl stretching modes and, since they are considerably red-shifted with respect to the carbonyl stretching frequency of the gas-phase formamide (1754 cm^{-1} [35]), they most probably relate to the molecule interacting with different sites/generating different adduct structures at the silica surface. In general, the possibility to probe acid surface sites with molecules containing the weakly basic carbonyl group is a well-established tool in the field of vibrational spectroscopy [36–38]. The interaction of the carbonyl group with the surface sites leads to a perturbation of its electronic structure, which produces a shift of its stretching mode strongly correlated to the strength of the interaction. Thus, the local structure of the surface sites and strength of their interaction with the probe molecule can be inferred [38]. In the same spectroscopic region, a weak and broad band ascribed to the NH_2 bending mode is observed (Figure 3b). At maximum coverage, it is centered at ~1605 cm^{-1} nd progressively red-shifts down to 1600 cm^{-1} upon outgassing. No clear components are revealed during formamide desorption as occurring for the carbonyl stretching band instead.

3.2 Simulation of formamide-A50 adducts

3.2.1 Low coverage models

In Table 1 the energetic values for the adsorption of formamide at low coverage on the SiO_2 surface are reported.

Table 1. Adsorption energies (ΔE^c, with explicit dispersive contributions reported in parentheses), enthalpies (ΔH^c) and Gibbs free energies (ΔG^c) for the SiO_2-formamide adducts low coverage models. The energy values are calculated according to equation 1) (*vide supra*). Interaction energy values (in kJ mol^{-1}) have been BSSE corrected through the counterpoise method. The last column shows the Boltzmann population ($p \leq 1$) calculated from the ΔG^c at STP conditions (298.15 K, 1 atm).

Model	ΔE^c (ΔE disp)	ΔH^c	ΔG^c	p
SiO_2-FA1	-69.9 (-18.8)	-62.8	-13.3	0.03
SiO_2-FA2	-44.0 (-28.1)	-38.1	8.6	0.00
SiO_2-FA3	-68.0 (-26.4)	-60.7	-9.6	0.01
SiO_2-FA4	-80.5 (-27.4)	-74.2	-21.3	0.67
SiO_2-FA5	-63.3 (-15.6)	-56.8	-19.3	0.30

Independently from the model (i.e. the type of formamide adduct at the SiO_2 surface), the adsorption process is exothermic, according to the negative values of ΔE^c and ΔH^c. Nevertheless, these values assume rather different values, in agreement with the variety of interactions formamide can establish with the surface. In all the cases (with the only exception of the SiO_2-FA2 model), the key interaction is represented by the H-bond from a silanol group at the surface and the carbonyl group of formamide. Additionally, the same structures further present a second H-bond interaction from the amine group of formamide toward siloxane bridges at the surface. For all considered structures, the NH_2 group always behaves as weak Brønsted acid and is never involved as a H-

Peer-reviewed version available at *Life* **2018**, *8*, 42; doi:10.3390/life8040042

acceptor group. Despite the analogous docking, the ΔE^c values are rather different among these four structures: an important parameter to be considered is the extent of the dispersive forces, as highlighted in Table 1. In fact, some of the adducts are strongly stabilized by this energetic term, e.g. SiO_2-FA3 and SiO_2-FA4: looking at the spatial relation between formamide and SiO_2 surface, in these models the molecules lean flat at the surface maximizing their dispersive interaction. Conversely, in models SiO_2-FA1 and SiO_2-FA5, dispersive interaction are lower according to the "perpendicular" arrangement of formamide with respect to SiO_2. As an example, a graphical comparison of adducts SiO_2-FA4 and SiO_2-FA5 are reported in Figure 4.

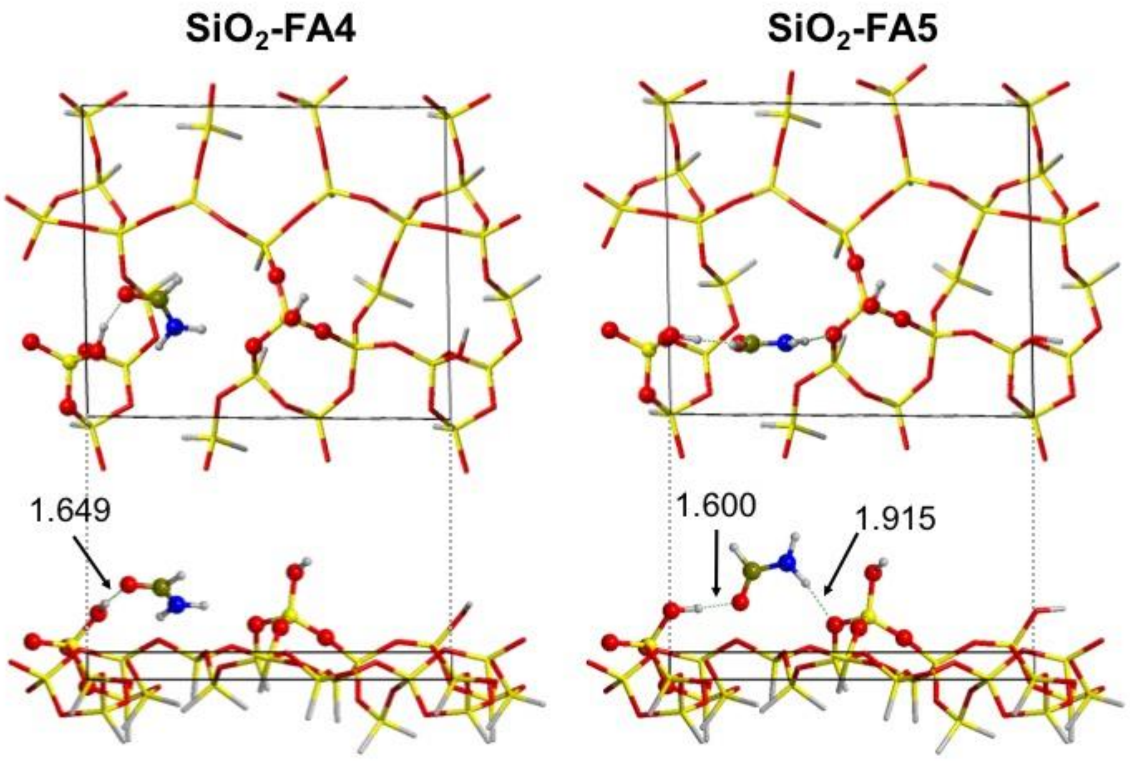

Figure 4. Top and side view of the most stable low coverage models, SiO_2-FA4 and SiO_2-FA5. Also shown are the relevant formamide-surface distances (in Å).

Finally, SiO_2-FA2 represent an extreme case, where the formamide-surface interaction can be considered barely dispersive, as the electronic component of ΔE^c accounts for less than 40% of the total. Interestingly, formamide establishes the stronger adducts (SiO_2-FA4) with the less exposed silanol group, most probably because of the easier formation of a weak H-bond between the amine group and a distorted Si-O-Si bridge (see Figure 4) and the efficient dispersive interaction due to the closer sitting of the molecule at the surface. The computed Gibbs free energies of interactions show the formation of adducts involving direct H-bonds as spontaneous. The lowest ΔG^c (stronger affinity) are achieved for the models where formamide interacts with the less exposed silanol (e.g. SiO_2-FA4 and SiO_2-FA5). Translating the Gibbs free energies to the probability of formation of each adduct on the basis of the Boltzmann distribution function, the latter accounts for the 97% of low coverage adsorption structures. Finally, the SiO_2-FA2 adduct in which no specific H-bond is present (see Figure S2 of the Supplementary Material) is the only case exhibiting a positive ΔG^c, testifying the key role of H-bond in making spontaneous the adsorption process.

3.2.2 High coverage models

A set of high coverage models has been generated by docking a second formamide molecule toward the previously considered structures in which one formamide was already pre-adsorbed. Their interaction energy, with respect to the most stable adduct at low coverage (i.e. SiO_2-FA4), has

Peer-reviewed version available at Life 2018, 8, 42; doi:10.3390/life8040042

been calculated. With respect to the low coverage situation, for the high coverage case a higher variability is possible. The second molecule can interact with the silanol not yet bound upon the first adsorption process, but at the same it can also establish a direct lateral interaction with the previously adsorbed formamide. In this case, a dimer-like adsorbed specie will be formed. Conversely, if the second molecule only interact with the surface without a direct involvement of the previously adsorbed one, a double-monomer adduct can be identified. Accounting for this further degree of freedom and for further orientations, a set of 7 high coverage structures has been built (of that, 3 are double monomers and 4 are dimers). The energetic parameter for the adsorption of the second formamide molecule are reported in Table 2. For the sake of comparison, the same energetic values, but computed for the direct adsorption of two formamide molecules over the pristine SiO_2 surface, are given in Table S13 of the Supplementary Material.

Table 2. Adsorption energies (ΔE^c, with explicit dispersive contributions reported in parentheses), enthalpies (ΔH^c) and Gibbs free energies (ΔG^c) for the SiO_2-formamide adducts high coverage models. The energy values are calculated according to equation 2) (*vide supra*). Energy values (in kJ mol^{-1}) have been BSSE corrected through the counterpoise method. The last column shows the Boltzmann population ($p \leq 1$) calculated from the ΔG^c at STP conditions (298.15 K, 1 atm).

Model	ΔE^c (ΔE disp)	ΔH^c	ΔG^c	p
SiO_2-2FA1	-57.6 (-28.4)	-50.1	-1.7	0.00
SiO_2-2FA2	-56.4 (-20.4)	-49.2	-6.3	0.01
SiO_2-2FA3	-67.3 (-16.9)	-59.9	-17.9	0.91
SiO_2-Dim1	-46.8 (-24.2)	-39.9	7.2	0.00
SiO_2-Dim2	-73.5 (-24.1)	-64.7	-12.0	0.08
SiO_2-Dim3	-51.7 (-19.3)	-43.4	2.3	0.00
SiO_2-Dim4	-58.5 (-21.3)	-49.4	-1.5	0.00

The adsorption of a second formamide molecule is exothermic for all considered high coverage structures, with average values of ΔE^c and ΔH^c just slightly lower than those for single adsorption (see Table 1). In detail, most of the adducts exhibit ΔE^c in the -45/-60 kJ mol^{-1} range, whereas only in two cases stronger interaction occurs (i.e. for the double monomeric SiO_2-2FA3 and the dimer-like SiO_2-Dim2 models). The structure of the latter is graphically reported in Figure 5.

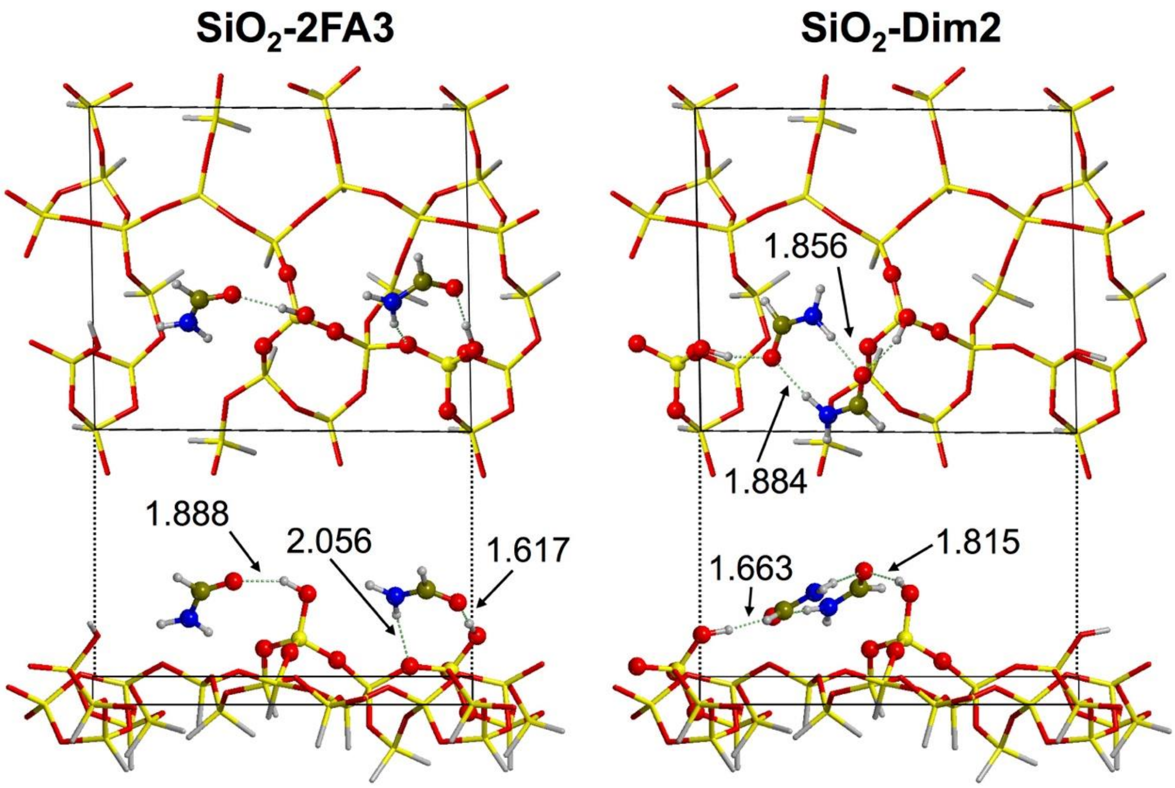

Figure 5. Top and side view of the most stable high coverage models, SiO_2-2FA3 and SiO_2-Dim2. Also shown are the relevant formamide-surface distances (in Å).

In the case of SiO_2-2FA3 double monomer adduct, each formamide molecule binds to a silanol group, forming a chain-like structure along the surface. The comparison with SiO_2-FA4, shows that the adsorption does not follow the Langmuir model, as the ΔG^c values are 21 and 18 kJ mol^{-1}, respectively. This indicate some sort of cooperativity between adsorption sites (as shown in Figure 5 for the SiO_2-2FA3 case) due to bridging interactions caused by the adsorbed formamide. Instead, in the SiO_2-Dim2 dimeric adduct the two formamide molecules interacts with a reciprocal orientation resembling the free dimer in gas phase. Moreover, further H-bonds are established between carbonyl groups and silanols, securing the dimeric structure to the surface. As previously commented for the SiO_2-FA4 low coverage adduct, in both the structures here described the formamide molecules lean almost flat at the surface, maximizing the dispersive interactions. Even if the SiO_2-2FA3 structure does not present the highest stability (SiO_2-Dim2 has higher ΔE^c and ΔH^c in absolute value), its ΔG^c value is the lowest, probably due to a larger entropic cost for SiO2-Dim2, due to the formation of the constrained dimeric structure. Therefore, the SiO_2-2FA3 Boltzmann population strongly dominates (91%) the HC case. It is worth noting, that the same Boltzmann population results when considering the ΔG^c values computed referring to the direct adsorption of two formamide molecules at the bare SiO_2 surface to yield the HC adducts (see data in Table S13 of the Supplementary Material).

3.3 Simulation of FTIR spectra of formamide-A50 adducts: comparison with experimental results

By means of the results for the model described in the previous paragraphs, a tentative interpretation of the experimental IR spectra has been carried out. The simulated spectrum for each adduct has been built by overlapping Gaussian functions whose main parameters (maximum position and intensity) have been estimated through a reduced Hessian frequency calculation. The frequencies have been scaled as described in Section 2.2. The full width at half maximum (FWHM) of Gaussian functions has been arbitrary set to 20 cm^{-1}. The overall simulated spectra have been computed by a linear combination of the spectra of each adduct (including only the single adducts for the LC case and, conversely, only double adducts in the case of HC), weighted by the corresponding Boltzmann populations (see Table 1 for LC and Table 2 for HC). The intensity of the

Peer-reviewed version available at Life 2018, 8, 42; doi:10.3390/life8040042

overall simulated spectra has been normalized to the maximum absorbance of the corresponding experimental reference spectra to facilitate the comparison. Results for such procedure are graphically outlined in Figure 6.

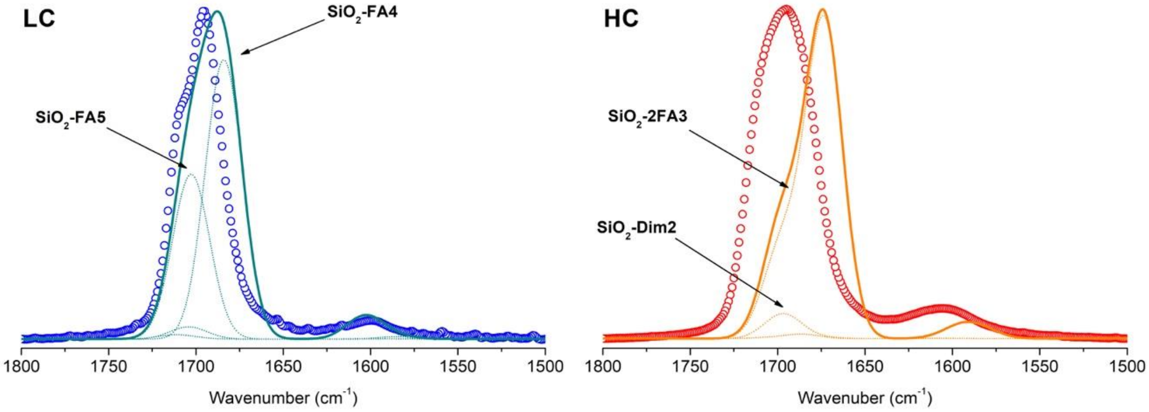

Figure 6. Reference experimental spectra at low coverage (LC, blue empty dots) and high coverage (HC, red empty dots) compared to the simulated ones (solid cyan and orange lines for LC and HC respectively). Simulated spectra have been reconstructed from the computed vibrational frequencies (spectral profiles described by Gaussian functions with FWHM of 20 cm^{-1}) for each LC/HC adduct weighted over the corresponding Boltzmann population. The single simulated spectral components (i.e. each belonging to a single adduct model) are reported as dotted lines for both LC and HC (nil components are omitted for clarity).

For the LC case, a nice qualitative agreement is found between the reference experimental spectrum and the simulated one. The clear bimodal shape of the absorption line in the experimental spectrum if effectively reproduced by modelling and the two observed spectral components can be assigned to specific formamide adducts at the silica surface as revealed by quantum mechanical simulation. In particular, the main feature peaked at 1695 cm^{-1} is assigned to the SiO_2-FA4 model (see Figure 4) with formamide interacting with the silanol group laying closer to the silica surface. The formamide molecule is further oriented with its symmetry plane parallel to the surface, thus maximizing the dispersive interaction. The high frequency shoulder of the peak (roughly centered at 1710 cm^{-1}) is instead ascribed to the SiO_2-FA5 adduct (see Figure 4), where formamide interacts with the same silanol taking part to the FA4 adduct, but with its symmetry plane perpendicular to the surface. The NH_2 bending mode feature at roughly 1600 cm^{-1} is well reproduced by simulation too, further validating the reliability of the combined experimental-simulation approach for the LC case.

In the HC case, a less satisfactory description of experimental outcomes is achieved by using spectral information from the simulation. The overall simulated spectrum (which is dominated by the contribution of SiO_2-2FA3 adduct) is too much red-shifted with respect to the experimental one, while components giving closer absorption frequencies (such as SiO_2-Dim2, the second adducts in terms of stability) are suppressed by the low value of their Boltzmann population. In detail, the maximum adsorption for the carbonyl stretching mode in the simulated spectrum is centered at 1675 cm^{-1}, thereby falling ~20 cm^{-1} below the experimental maximum. A similar red-shift also resulted for the NH_2 bending. However, the line-shape of the simulated carbonyl peak closely resembles the experimental one, with a clear shoulder falling at higher frequencies with respect to the peak maximum. Since the main difference between simulated and experimental spectrum is represented by a frequency offset, it may be possible that such discrepancy derives from a wrong scaling of the calculated frequency when formamide experiences multiple interactions (like in the HC case). Still, the possibility more complex adsorption structures (e.g. involving “liquid like” and or multiple layers of formamide) are involved at HC cannot be excluded a priori.

4. Conclusions

Peer-reviewed version available at *Life* **2018**, *8*, 42; doi:10.3390/life8040042

The adsorption of formamide on a silica characterized by low hydroxylation (about 1.5 silanol groups/nm^2) has been investigated through a combined experimental-simulation approach, in which experimental IR spectroscopic features have been interpreted by means of a quantum mechanical modeling study carried out on a realistic amorphous silica slab model. The IR spectra showed a lowering of the C=O stretching frequency, a clear indication of a H-bond interaction between isolated silanol groups and adsorbed formamide. Nonetheless, the C=O stretching band has a squat-like shape, clearly indicating a rather complex scheme of interaction with formamide molecules, not easily interpreted on a single kind of adsorption site, despite the nature of isolated silanol groups at the considered surface. A possible explanation of the observed spectral features has been provided by the computer modeling results, in which the adopted surface silica model exhibits two isolated silanol groups with different spatial accessibility and surrounding. Adsorption of formamide has been simulated by docking formamide towards the silica surface model in a step-wise approach, from low (LC: 1 formamide per unit cell) to high coverage (HC: 2 formamide per unit cell). A rather ample number of interaction cases have been studied, all of them fully characterized as far as optimum structures, Gibbs free energy of adsorption and vibrational spectra in the harmonic approximation. Analysis of the results revealed that H-bond interaction is the leading component of the interaction energy. However, dispersion interaction is always a significant component of the final interaction energy and cannot be ignored in calculations of this kind. Interestingly, cases in which H-bond is absent and the interaction is exclusively dominated by dispersion component exhibits positive Gibbs free energy of adsorption (unbound case). The infrared spectrum in the C=O and NH_2 region was simulated using the computed harmonic frequencies and intensities through a Boltzmann weighted sum of associated Gaussian-type functions to simulate the natural band width. For the LC case, a remarkably good agreement with the experimental spectrum was achieved. Far less satisfactory was the reconstruction of the HC spectrum. Reasons for that may be the insufficient coverage attained by the simple HC cases or even the simple scaling of the C=O and NH_2 frequencies not accounting for H-bond.

The present results allow to extend this study to the role of silica in the chemical reactivity of formamide, i.e. its decomposition in HCN and H_2O, a crucial step for the further chemical evolution towards nucleic base synthesis. Studies, both experimental and computational along that direction, are already in place in our laboratory.

Supplementary Materials: The following are available online at www.mdpi.com/xxx/s1, Figure S1 to S12: graphical details of the 12 formamide adsorption models, Table S1 to S12: key structural and spectroscopic features for the 12 formamide adsorption models, Table S13: Adsorption energies, enthalpies and Gibbs free energies for the SiO_2-formamide adducts high coverage models generated by double adsorption over the pristine SiO_2 surface.

Funding: "This research was funded by MIUR through the PRIN2015 project "STARS in the CAOS", grant number 2015F59J3R"

Acknowledgments:

Conflicts of Interest: The authors declare no conflict of interest.

References

1. Whitesides, G.M., Reinventing chemistry. *Angew. Chem. Int. Ed.* **2015**, *54*, 3196–3209.
2. Kahane, C.; Ceccarelli, C.; Faure, A.; Caux, E., Detection of formamide, the simplest but crucial amide, in a solar-type protostar. *Astrophys. J.* **2013**, *763*, L38.
3. Saladino, R.; Crestini, C.; Neri, V.; Brucato, J.R.; et al., Synthesis and Degradation of Nucleic Acid Components by Formamide and Cosmic Dust Analogues. *ChemBioChem* **2005**, *6*, 1368–1374.
4. Saladino, R.; Botta, G.; Bizzarri, B.M.; Di Mauro, E.; et al., A Global Scale Scenario for Prebiotic Chemistry: Silica-Based Self-Assembled Mineral Structures and Formamide. *Biochemistry* **2016**, *55*, 2806–

Peer-reviewed version available at *Life* **2018**, *8*, 42; doi:10.3390/life8040042

2811.

5. Saladino, R.; Crestini, C.; Costanzo, G.; DiMauro, E., Advances in the prebiotic synthesis of nucleic acids bases: Implications for the origin of life. *Curr. Org. Chem.* **2004**, *8*, 1425–1443.
6. Rotelli, L.; Trigo-Rodríguez, J.M.; Moyano-Cambero, C.E.; Carota, E.; et al., The key role of meteorites in the formation of relevant prebiotic molecules in a formamide/water environment. *Sci. Rep.* **2016**, *6*, 38888.
7. Senanayake, S.D.; Idriss, H., Photocatalysis and the origin of life: Synthesis of nucleoside bases from formamide on TiO2(001) single surfaces. *Proc. Natl. Acad. Sci. U. S. A.* **2006**, *103*, 1194–1198.
8. Saladino, R.; Crestini, C.; Neri, V.; Ciciriello, F.; et al., Origin of informational polymers: The concurrent roles of formamide and phosphates. *ChemBioChem* **2006**, *7*, 1707–1714.
9. Saladino, R.; Crestini, C.; Pino, S.; Costanzo, G.; et al., Formamide and the origin of life. *Phys. Life Rev.* **2012**, *9*, 84–104.
10. Saladino, R.; Crestini, C.; Costanzo, G.; Negri, R.; et al., A possible prebiotic synthesis of purine, adenine, cytosine, and 4(3H)-pyrimidinone from formamide: Implications for the origin of life. *Bioorganic Med. Chem.* **2001**, *9*, 1249–1253.
11. Muir, J.M.R.; Idriss, H., Formamide reactions on rutile TiO2(011) surface. *Surf. Sci.* **2009**, *603*, 2986–2990.
12. Kubelík, P.; Michal, R.; Shestivská, V.; Sponer, J.E., Correction for Ferus et al., High-energy chemistry of formamide: A unified mechanism of nucleobase formation. *Proc. Natl. Acad. Sci.* **2015**, *112*, E339–E339.
13. Rimola, A.; Costa, D.; Sodupe, M.; Lambert, J.F.; et al., Silica surface features and their role in the adsorption of biomolecules: Computational modeling and experiments. *Chem. Rev.* **2013**, *113*, 4216–4313.
14. Rimola, A.; Fabbiani, M.; Sodupe, M.; Ugliengo, P.; et al., How Does Silica Catalyze the Amide Bond Formation under Dry Conditions? Role of Specific Surface Silanol Pairs. *ACS Catal.* **2018**, *8*, 4558–4568.
15. Lambert, J.F., Adsorption and polymerization of amino acids on mineral surfaces: A review. *Orig. Life Evol. Biosph.* **2008**, *38*, 211–242.
16. Lambert, J.-F.; Jaber, M.; Georgelin, T.; Stievano, L., A comparative study of the catalysis of peptide bond formation by oxide surfaces. *Phys. Chem. Chem. Phys.* **2013**, *15*, 13371–80.
17. Martra, G.; Deiana, C.; Sakhno, Y.; Barberis, I.; et al., The formation and self-assembly of long prebiotic oligomers produced by the condensation of unactivated amino acids on oxide surfaces. *Angew. Chem. Int. Ed.* **2014**, *53*, 4671–4674.
18. Corno, M.; Delle Piane, M.; Monti, S.; Moreno-Couranjou, M.; et al., Computational Study of Acidic and Basic Functionalized Crystalline Silica Surfaces as a Model for Biomaterial Interfaces. *Langmuir* **2015**, *31*, 6321–6331.
19. Musso, F.; Sodupe, M.; Corno, M.; Ugliengo, P., H-bond features of fully hydroxylated surfaces of crystalline silica polymorphs: A periodic B3LYP study. *J. Phys. Chem. C* **2009**, *113*, 17876–17884.
20. Garofalini, S.H., Molecular dynamics computer simulations of silica surface structure and adsorption of water molecules. *J. Non. Cryst. Solids* **1990**, *120*, 1–12.
21. Tosoni, S.; Civalleri, B.; Pascale, F.; Ugliengo, P., Hydroxylated crystalline edingtonite silica faces as models for the amorphous silica surface. *J. Phys. Conf. Ser.* **2008**, *117*.
22. Tielens, F.; Gervais, C.; Lambert, J.F.; Mauri, F.; et al., Ab initio study of the hydroxylated surface of amorphous silica: A representative model. *Chem. Mater.* **2008**, *20*, 3336–3344.
23. Ugliengo, P.; Sodupe, M.; Musso, F.; Bush, I.J.; et al., Realistic models of hydroxylated amorphous silica surfaces and MCM-41 mesoporous material simulated by large-scale periodic B3LYP calculations. *Adv. Mater.* **2008**, *20*, 4579–4583.
24. Delle Piane, M.; Corno, M.; Ugliengo, P., Does dispersion dominate over H-bonds in drug-surface

Peer-reviewed version available at *Life* **2018**, *8*, 42; doi:10.3390/life8040042

interactions? The case of silica-based materials as excipients and drug-delivery agents. *J. Chem. Theory Comput.* **2013**, *9*, 2404–2415.

25. Mardyukov, A.; Sánchez-Garcia, E.; Rodziewicz, P.; Doltsinis, N.L.; et al., Formamide dimers: A computational and matrix isolation study. *J. Phys. Chem. A* **2007**, *111*, 10552–10561.
26. Alessandrini, S.; Puzzarini, C., Structural and Energetic Characterization of Prebiotic Molecules: The Case Study of Formamide and Its Dimer. *J. Phys. Chem. A* **2016**, *120*, 5257–5263.
27. Erba, A.; Baima, J.; Bush, I.; Orlando, R.; et al., Large-Scale Condensed Matter DFT Simulations: Performance and Capabilities of the CRYSTAL Code. *J. Chem. Theory Comput.* **2017**, *13*, 5019–5027.
28. Dovesi, R.; Erba, A.; Orlando, R.; Zicovich-Wilson, C.M.; et al., Quantum-mechanical condensed matter simulations with CRYSTAL. *Wiley Interdiscip. Rev. Comput. Mol. Sci.* **2018**, *8*, e1360.
29. Perdew, J.P.; Burke, K.; Ernzerhof, M., Generalized gradient approximation made simple. *Phys. Rev. Lett.* **1996**, *77*, 3865–3868.
30. Nada, R.; Nicholas, J.B.; McCarthy, M.I.; Hess, A.C., Basis sets for ab initio periodic Hartree-Fock studies of zeolite/adsorbate interactions: He, Ne, and Ar in silica sodalite. *Int. J. Quantum Chem.* **1996**, *60*, 809–820.
31. Schäfer, A.; Huber, C.; Ahlrichs, R., Fully optimized contracted Gaussian basis sets of triple zeta valence quality for atoms Li to Kr. *J. Chem. Phys.* **1994**, *100*, 5829–5835.
32. Antony, J.; Grimme, S., Density functional theory including dispersion corrections for intermolecular interactions in a large benchmark set of biologically relevant molecules. *Phys. Chem. Chem. Phys.* **2006**, *8*, 5287–5293.
33. Dovesi, R.; Saunders, V.R.; Roetti, C.; Orlando, R.; et al., CRYSTAL17 User's Manual. **2017**.
34. Lendvay, G.; Mayer, I., Some difficulties in computing BSSE-corrected potential surfaces of chemical reactions. *Chem. Phys. Lett.* **1998**, *297*, 365–373.
35. Sugawara, Y.; Hamada, Y.; M., T., Vibration-rotation Spectra of Formamide. *Bull. Chem. Soc. Jpn.* **1983**, *56*, 1045–1050.
36. Crocellà, V.; Cerrato, G.; Magnacca, G.; Morterra, C., Adsorption of Acetone on Nonporous and Mesoporous Silica. *J. Phys. Chem. C* **2009**, *113*, 16517–16529.
37. Crocellà, V.; Cerrato, G.; Morterra, C., On the adsorption/reaction of acetone on pure and sulfate-modified zirconias. *Phys. Chem. Chem. Phys.* **2013**, *15*, 13446.
38. Lamberti, C.; Zecchina, A.; Groppo, E.; Bordiga, S., Probing the surfaces of heterogeneous catalysts by in situ IR spectroscopy. *Chem. Soc. Rev.* **2010**, *39*, 4951.